Quaternary International 253 (2012) 55–66

Contents lists available at ScienceDirect

Quaternary International

journal homepage: www.elsevier.com/locate/quaint

Mid-Holocene mean climate in the south eastern Pacific and its influence on South America

Matthieu Carré [a,*], Moufok Azzoug [a], Ilhem Bentaleb [a], Brian M. Chase [a,b], Michel Fontugne [c], Donald Jackson [d], Marie-Pierre Ledru [h], Antonio Maldonado [e], Julian P. Sachs [f], Andrew J. Schauer [g]

[a] Institut des Sciences de l'Evolution de Montpellier, UMR5554, CNRS/Université Montpellier 2, CC061, Pl. Eugène Bataillon, 34095 Montpellier, France
[b] Department of Archaeology, History, Culture and Religion, University of Bergen, Postbox 7805, 5020 Bergen, Norway
[c] Laboratoire des Sciences du Climat et de l'Environnement, UMR CEA/CNRS 1572, Domaine du CNRS, 91198 Gif-sur-Yvette cedex, France
[d] Departamento de Antropología, Facultad de Ciencias Sociales, Universidad de Chile, Ignacio Carrera Pinto, 1045 Ñuñoa, Santiago, Chile
[e] Centro de Estudios Avanzados en Zonas Áridas, Universidad de La Serena, Chile
[f] University of Washington, School of Oceanography, Box 355351, Seattle, WA 98195, USA
[g] University of Washington, Department of Earth and Space Sciences, Box 351310, Seattle, WA 98195, USA
[h] IRD – UMR 203, Institut des Sciences de l'Evolution de Montpellier, Université Montpellier 2, CC061, Pl. Eugène Bataillon, 34095 Montpellier, France

ARTICLE INFO

Article history:
Available online 19 February 2011

ABSTRACT

The eastern tropical Pacific plays a key role in the tropical atmospheric circulation and in the global carbon cycle, and assessing the sensitivity of this region to global climate changes is a major challenge facing climatologists. Provided here is a synthesis of proxy records of the mean climate of the mid-Holocene (5–8 ka) along the south eastern Pacific margin and four regions of South America. These regions were selected for the strength and stability of ENSO teleconnections, and located outside the direct influence of the intertropical convergence zone or the southern westerlies in order to avoid the overprinting signal of their insolation-related variations and focus on the relationship between the eastern tropical Pacific and South America. This study is based on a review of published multiproxy data as well as new isotopic data from the Peruvian and Chilean coast. The available evidence indicates that sea-surface temperatures were ~1–4 °C cooler from the Galapagos to the southern Peruvian coast as a result of increased coastal upwelling forced by changes in longshore windfields. The mean La Niña-like conditions in the eastern South Pacific were associated to aridity in southern Brazil and along the whole South American Pacific coast from central Chile to the Galapagos, and to wetter conditions on the western central Andes. This regional synthesis provides a coherent picture of the South American mean climate that is very similar to the modern precipitation pattern observed during La Niña conditions, suggesting that atmospheric teleconnections linking the South Eastern Pacific to these continental areas were similar in the middle Holocene.

© 2011 Elsevier Ltd and INQUA. All rights reserved.

1. Introduction

South America, with a latitudinal range from 12°N to 56°S, is a continental bridge between low and high latitudes in the Southern Hemisphere, where Walker and Hadley circulations are strongly affected by land–ocean–atmosphere feedbacks (Aceituno, 1988; Mitchell and Wallace, 1992; Takahashi and Battisti, 2007; Garreaud et al., 2009, and references therein). This region plays a major role in the global carbon cycle through the Amazon forest and upwelling-induced marine productivity. Understanding the response of the Southeast Pacific–South America boundary to global climate change is thus a major challenge facing climatologists.

Today, El Niño phases are characterized by a deepening of the thermocline in the eastern Pacific resulting in warm sea-surface temperatures (SSTs) anomalies from the eastern equatorial Pacific down to central Chile. Deep atmospheric convection is increased over the central and eastern equatorial Pacific, the Intertropical Convergence Zone (ITCZ) is shifted southward toward the equator, bringing more precipitation to the Galapagos and the northern Peruvian coast. An opposite effect is observed in the Andes Altiplano, with generally drier conditions during El Niño anomalies (Garreaud, 1999; Lenters and Cook, 1999), especially in the western Altiplano (Vuille et al., 2000). The weakening of the subtropical anticyclone weakens the wind stress along the South American

* Corresponding author.
E-mail address: matthieu.carre@univ-montp2.fr (M. Carré).

1040-6182/$ – see front matter © 2011 Elsevier Ltd and INQUA. All rights reserved.
doi:10.1016/j.quaint.2011.02.004

Pacific coast, thus reducing coastal upwelling. This also results in increased winter precipitation on the central Chilean coast. During El Niño phases, cyclonic anomalies occur over south eastern South America related to Walker and Hadley circulations anomalies originating in the eastern Pacific (Grimm, 2003). They favour moisture incursions from the Atlantic from October through May, increasing significantly the annual precipitation in southern Brazil, Uruguay and northern Argentina (Garreaud et al., 2009; Grimm and Tedeschi, 2009). A comprehensive review of the modern South American climate and oceanic influences can be found in Garreaud et al. (2009). In summary, El Niño phases are characterized by increased moisture in three of the selected areas (Galapagos, Central Chilean coast and South eastern Brazil) and drier condition in the fourth selected area, western central Andes. La Niña episodes have largely opposing signatures. This paper compares the mid-Holocene mean conditions to these patterns, in order to have a better understanding of the past tropical Pacific mean dynamics and its influence on the South American climate, keeping in mind a globally different climatic context.

During the mid-Holocene (5–8 ka), a period considered to be a "Climatic Optimum" in the northern hemisphere, significant climate changes have been recorded worldwide. In intertropical South America, in response to low latitude direct insolation forcing, the mean position of the ITCZ is thought to have been further north and the South American monsoon was weaker than it is today (Haug et al., 2001; Fleitmann et al., 2003; Cruz et al., 2005; Wang et al., 2005). The Subtropical Front and the southern westerlies seemed also shifted poleward, bringing less humidity to the southernmost South America (Lamy et al., 2001; Verleye and Louwye, 2010). However, considering the wide-ranging teleconnections associated with the tropical Pacific it is important to determine long-term variations in the region mean state. Ongoing debates about this variability, particularly during the mid-Holocene, result largely from the contradictory proxy records from the eastern tropical Pacific. This paper addresses this question with new proxy data for coastal SST in the Chile–Peru upwelling system, and a synthesis of the available oceanic datasets. The reconstructed southeast Pacific paleoceanographic pattern was compared to rainfall-related proxy data from four related regions of South America: 1) the Galapagos Islands, coastal Ecuador and the northern Peruvian coast, 2) the central Chilean coast, 3) South eastern Brazil to northeastern Argentina, and 4) the western slope of the central Andes. These regions were selected because: 1) strong and stable atmospheric teleconnections with the tropical Pacific have been identified (Aceituno, 1988; Aceituno and Montecinos, 1993; Grimm et al., 2000; Montecinos et al., 2000; Montecinos and Aceituno, 2003; Grimm and Tedeschi, 2009), and 2) they are located outside the direct influence of the South American Summer Monsoon and the southern westerlies, thus avoiding as much as possible the overprinting signal of their insolation-related variations. This approach was designed in order to get insights into the mid-Holocene atmospheric teleconnections between the eastern tropical Pacific and South America.

2. Paleoceanographic data from mollusc shell stable isotopes

2.1. Sites

Fossil shells of the bivalve *Mesodesma donacium* were collected from three archaeological sites along the Peruvian and the Chilean coast (Table 1). The occupation levels were radiocarbon dated using fragments of mollusc shell, or charcoal when it was possible. Modern shell samples were collected from adjacent beaches for a modern reference.

The Rio Ica site has been described by Engel (1957). It is located on the northern side of the Rio Ica, very close to the river mouth. Fossil shells and charcoal fragments were collected at the surface of the shell mound. Today, the river is not permanent but maintains some vegetation in the middle of an extremely arid desert. This area lies in the core of the most intense upwelling cell along the Peruvian coast. Rainfall is virtually nonexistent (<10 mm/y) and not significantly affected by ENSO events.

The Quebrada de los Burros (QLB) is a pre-ceramic site from southern Peru excavated by the Perou-Sud project between 1995 and 2008. It was occupied almost continuously from c. 10 ka to c. 6.5 ka (Lavallée et al., 1999; Carré et al., 2009). The shell sample analysed here was collected in the uppermost level (N2). Coastal fogs that form during the cold season between June and November are presently the main source of humidity in the very arid environment. Intense and very short rainfall events (~1–2 days) may occur occasionally (but not systematically) as a result of El Niño events. Such events are too short to affect significantly the sea water isotopic composition on a monthly timescale.

The Los Vilos archaeological sites are located on the semi-arid coast of Central Chile. LV098 is an important site that was continuously occupied during several centuries in the early Holocene (~9.9 ka). It was excavated by Donald Jackson who collected mollusc shells and charcoals in successive stratigraphic levels (Jackson and Méndez, 2005). LV158 is a more recent (~4.5 ka) and ephemeral site. Despite the range of radiocarbon dates, the size of the site suggests that it was probably not occupied more than a decade. Precipitation occurs mainly between June and August with an annual total of about 100–200 mm. However, rainfall in this area is highly variable, being related to the El Niño-Southern Oscillation (ENSO), with positive (negative) precipitation anomalies during El Niño (La Niña) years (Aceituno, 1988).

2.2. Material and methods

M. donacium is a bivalve living in the intertidal to subtidal zone of the sandy beaches in Chile and Peru. Shell accumulation rarely exceeds 3–4 years. Only shells longer than 60 mm were analysed, so at least a full annual cycle was recorded. Scanning electronic microscope analyses showed that the shell inner organic matter was preserved in the Peruvian shells, which guarantees that the aragonite geochemistry was not altered. The state of preservation of the organic matrix in the Chilean shells was not as good because of the less arid environmental conditions, but the aragonite crystals microstructure appeared to have been preserved nevertheless. Shells were embedded in polyester resin and radially sectioned with a low speed diamond wire saw. Sections 1 mm thick were polished and microsampled using an automated microdrill. This technique allows avoidance of locally altered areas of the outer surface. This species forms tide-related fortnightly growth line clusters that can be used as a calendar (Carré et al., 2005a; Carré, 2007). Each microsample (~100 μg of aragonite powder) crossed two consecutive fortnightly cycles so that it averages conditions over about a month. Thus, each shell provided a 1–3 year record resolved to monthly timescales, except for the shells from the Chilean sites LV158 and LV098 from which only one single sample averaging the full shell lifetime was taken. The number of shells analysed in each site is reported in Table 1.

Oxygen stable isotope ratios were measured at the Vrije Universiteit of Amsterdam using a Finnigan Delta+ mass spectrometer coupled to a Gasbench II continuous flow system (analytical precision better than 0.12‰) and at the University of Washington Isolab using a Finnigan Delta+ mass spectrometer coupled to a Kiel III carbonate device (analytical precision better than 0.08‰). Mass spectrometers were calibrated using NBS19 and NBS18 IAEA

Table 1
Coastal sites studied for mollusc shell stable isotopes.

Site	Location	Period[a]	Level	^{14}C dates	Dated material	Lab reference	Cal. range (1σ), yr BP[b]	Number of shells analysed	N; $N_w + N_s$[c]	Ice volume δ^{18}O correction[d]
Rio Ica	14°52′ S; 75°34′W	Modern						15	25.5; 26w + 25s	0
		MH	Surface	5840 ± 35	Charcoal	OS-60543	6530–6900	20	28; 24w + 32s	−0.05 ± 0.02
				5900 ± 40	Charcoal	OS-60564				
				5940 ± 45	Charcoal	OS-60556				
				6070 ± 30	Charcoal	OS-60544				
QLB	18°1′S; 70°50′W	Modern						17	19.5; 19w + 20s	0
		MH	N2	6050 ± 80	Charcoal	Missing	6730–7560	14	15; 14w + 16s	−0.09 ± 0.02
				6460 ± 60	Charcoal	GIF9-97287				
				6510 ± 60	Charcoal	GIF9-97288				
				6630 ± 70	Charcoal	GIF9-97289				
Los Vilos	31°52′S; 71°31′W	Modern						5	6.5; 6w + 7s	0
		MH	LV158, N1-N5	4540 ± 40	Mollusc	OS-63178	4340–4650	5	5	0
				4610 ± 40	Mollusc	OS-63179				
		EH	LV098B, N7-N15	8620 ± 110	Charcoal	OS-61907	9460–10,380	5	5	−0.31 ± 0.05
				8690 ± 40	Charcoal	OS-60542				
				9190 ± 45	Charcoal	OS-61906				

[a] MH: Mid-Holocene, EH: Early Holocene.
[b] Calibration was performed using CALIB program (Stuiver and Reimer, 1993), version 5.0.1. The SHCal04 calibration dataset (Mc Cormac et al., 2004) was used for charcoal, and the Marine04 calibration dataset (Hughen et al., 2004) was used for molluscs, with a regional reservoir effect of $\Delta R = 226 \pm 70$ (Ortlieb et al., 2011).
[c] Total number of years recorded by the shell sample, number of winters (w) + number of summers (s).
[d] Based on Lambeck and Chappell (2001).

standards in order to have isotopic ratios (δ^{18}O notation) expressed on the V-PDB scale. Isotopic values were averaged for each site and period so that mean conditions could be compared.

2.3. Reconstructing sea-surface temperature (SST) changes

Mollusc shell aragonite δ^{18}O is related to the water temperature and the water δ^{18}O through a nearly linear relationship (Epstein et al., 1953; Grossman and Ku, 1986). The sea water δ^{18}O on the South Peruvian coast is not affected by freshwater inputs because of the strong aridity so that shell δ^{18}O variations in shells would only reflect temperature variations. Although the central Chilean coast experiences more rainfall than the Peruvian coast, a weekly one-year long monitoring of the sea water δ^{18}O showed no significant seasonal fluctuation. The monthly standard deviation of the sea water δ^{18}O, likely related to local evaporation, was estimated at ~0.1‰ ($n = 52$). The good correlation between SST and shell δ^{18}O was demonstrated for *M. donacium* comparing the isotopic record of live-collected shells with SST instrumental records (Fig. 1) (Carré et al., 2005a). These authors found that, assuming a constant value of the sea water δ^{18}O, a 1‰ deviation in the *M. donacium* shell δ^{18}O represents a temperature change of 3.66 °C, whereas it would represent 4.34 °C according to the widely used equation of Grossman and Ku (1986).

At millennial timescales, the isotopic effect of the polar ice sheets must also be considered. An ice volume correction was applied based on Lambeck and Chappell (2001) (Table 1). The systematic error related to the mean ocean δ^{18}O variations was estimated as within the range of the age uncertainty (Table 1). Annual mean sea water δ^{18}O in a locality might also vary over long timescales because of ocean circulation changes. These advection changes could bring fresher water from the high latitudes, or saltier water from the South Pacific subtropical gyre. In the area of study, a 500 km displacement of salinity gradients would represent less than 0.3 salinity units (based on Levitus Atlas 1994), equivalent to ~0.14‰ change of the water δ^{18}O (Delaygue et al., 2000). This value was added to the systematic error bar of fossil shell samples (Fig. 2).

Mean annual conditions were estimated by averaging annual isotopic mean values from individual shells. The statistical error bar of the estimated mean value depends on the sample size (i.e. the number of shells), the climate variability, and several stochastic uncertainties acting at different timescales, so that the error bar cannot be estimated by simple sampling statistics. The statistical error bar of reconstructed mean annual values was estimated using a Monte Carlo simulation. The Puerto Chicama instrumental SST timeseries from 1925 to 2002 (http://jisao.washington.edu/data_sets/chicama_sst/), was used centered and converted to δ^{18}O variations using a slope value of 3.66°C/‰ (Carré et al., 2005a). Shell δ^{18}O records were modelled as 1-year long monthly windows (January–December) randomly extracted from the Puerto Chicama calculated δ^{18}O timeseries, disturbed by statistical noises to simulate the proxy uncertainties: (i) a normally distributed annual noise representing the coastal temperature heterogeneity with a standard deviation of 0.4‰ equivalent to 1.5 °C in temperature, and (ii) a normally distributed monthly noise with a standard deviation of 0.2‰, corresponding to the sea water δ^{18}O monthly variability (0.16‰) combined in quadrature with the analytical error (0.1‰). The standard error of the reconstructed mean value from a sample of shells recording N_{yrs} years was estimated by the standard deviation of 1000 repeated sampling. As expected the error bar decreases rapidly with the sample size (Fig. 1E). For every sample, N_{yrs} is the sum of the number of years recorded by every shell (Table 2). Finally, the total error bar is the sum of the systematic error (ice volume effect uncertainty + potential advective change) and the statistical error (Fig. 2).

2.4. Results

New isotopic results obtained from *M. donacium* shells are summarized in Table 2. Mid-Holocene isotopic mean values are significantly more positive (95% confidence level) from 14°S (Rio Ica) to 18°S (QLB), indicating cooler conditions than today (Fig. 2). This result confirms the earlier findings of Carré et al. (2005b). In Central Chile, conditions are similar to today in the early Holocene and also cooler just after the mid-Holocene. SST changes were approximately −0.7 °C (±0.9 °C) in Rio Ica, −4.5 °C (±1.1 °C) in QLB, and −0.9 °C (±1.4 °C) in Los Vilos at 4.5 ka, based on the Carré et al. (2005a) equation. Grossman and Ku's (1986) equation would yield larger SST differences.

In addition to these new results, shell stable isotope results from the Siches (Nicholas, 1996; Houk, 2002) and Ostra (Perrier et al.,

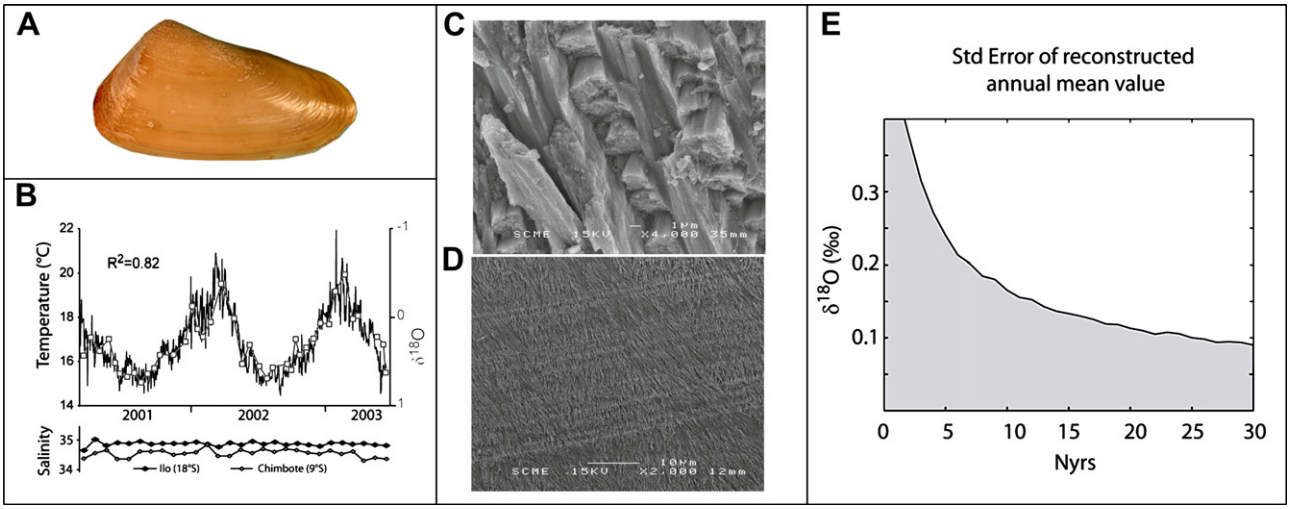

Fig. 1. A: *Mesodesma donacium* shell. B: $\delta^{18}O$ profile in a modern shell compared to local SSTs (adapted from Carré et al., 2005a) and salinity from Ilo and Chimbote measured by IMARPE. C: SEM view of the aragonite cross lamellar dense microstructure in the outer layer of a fossil *M. donacium* shell from QLB. D: same as C with a polished and etched surface. Organic matrix fibers appear perfectly preserved. The cross lamellar structure and the growth lines are apparent. E: Standard error of the mean SST-related $\delta^{18}O$ fractionation vs. the number of years recorded in a shell sample, calculated with a Monte Carlo simulation.

1994; Nicholas, 1996; Houk, 2002) archaeological sites are included. Based on the results of these authors (Table 3), annual mean values in the mid-Holocene were enriched by ~1.2‰ at Siches and ~1.6‰ at Ostra (Fig. 2). At Siches, where monsoon rainfalls occur from January to March, these values indicate significantly cooler and/or drier conditions. At Ostra, these values could either be related to cooler mid-Holocene conditions or to highly evaporative lagoon conditions as suggested by geomorphologic studies (De Vries and Wells, 1990; Perrier et al., 1994). Such results are in contradiction with the conclusions of Sandweiss and Richardson (1996) and Andrus et al. (2002) based on anomalous mollusc assemblages and fish otoliths stable isotopes, respectively.

3. Data synthesis

This section considers oceanic and continental paleoclimate records in an attempt to establish a coherent idea of the mean climate in the mid-Holocene, focusing on the influence of the south eastern Pacific on South America's average precipitation regime. Reported in Table 4 and Fig. 3 are the available marine records from this area that could provide reliable information regarding SSTs and upwelling intensities during the mid-Holocene. In collating these data, preference was given to well-dated marine and continental sediment cores with time resolution better than 500 years were selected. In the Andes, the Pacific influence is much more predominant on the western slope than in the eastern Altiplano (Vuille et al., 2000). Sites from the high and eastern Andean Altiplano were excluded because of the heterogeneity of local climate conditions and the strong influence of the Amazon basin that would mask the background Pacific influence. Rainfall in northeastern Brazil rainfalls, while being strongly influenced by SSTs in the tropical Pacific, was excluded because it lies in the core of the ITCZ seasonal migration (Grimm, 2003). Therefore, the ITCZ latitudinal shift observed in the South American tropics at the Holocene (Haug et al., 2001) would overwhelm potential changes related to the tropical Pacific. Of course, paleoclimate proxy records from the four selected continental regions cannot be simply interpreted as El Niño-like or La Niña-like patterns, as the ITCZ does have a climatic influence on Ecuador and Southern Brazil as well as the southern westerlies have an influence on central Chile and Argentina. Nevertheless, these regions were selected because they would provide the highest signal to noise ratio to study the tropical Pacific influence over millennial timescales. Instrumental rainfall dataset analyses showed that southern Brazil had the most intense subtropical ENSO teleconnection (Grimm et al., 2000). The ENSO teleconnection in Central Chile seems the more stable on decadal scales (Aceituno and Montecinos, 1993). The highest rainfall sensitivity to the eastern Pacific SSTs is found in the Galapagos Islands. In these three regions selected, El Niño (La Niña)-like anomalies induce increased (decreased) precipitation. Conversely, the western slope of central Andes experiences drier conditions during El Niño phases and more humidity during La Niña phases (Garreaud, 1999; Lenters and Cook, 1999).

4. Discussion

4.1. Eastern tropical Pacific

From the eastern equatorial Pacific to southern Peru, most marine records indicate cooler conditions, suggesting a shallower thermocline and a strengthened Walker circulation. This is consistent with lower lake level recorded in the Galapagos Islands (Colinvaux, 1972), since cool oceanic conditions tend to decrease coastal rainfall. Two studies based on fossil mollusc assemblages (Sandweiss, 1986) and fish otolith $\delta^{18}O$ (Andrus et al., 2002) propose an opposite scenario for the Peruvian coast and are at the centre of an old controversy. Mangroves have disappeared today from Siches, northern Peru (Figs. 2 and 3). Their presence, revealed by mollusc remains in the mid-Holocene, was interpreted by Sandweiss (1986) and Sandweiss and Richardson (1996) as indicating warmer and moister conditions. However, a mangrove ecosystem still exists further south (5°30'S) near Sechura (Barrionuevo and Marcial, 2006), in drier and cooler conditions than prevail in Siches, suggesting that mangrove could have grown at the site in mid-Holocene, even in a drier environment. Andrus et al. (2003) argued – in response to Béarez et al. (2003) – that the depleted values of oxygen isotopes recorded in fish otoliths from Siches reflect warmer conditions and could not be due to fish incursions into estuaries because there are no real estuaries in this part of the Peruvian coast. However, the coastal conditions were different at 7 ka when the sea level was ~1 m higher than today in

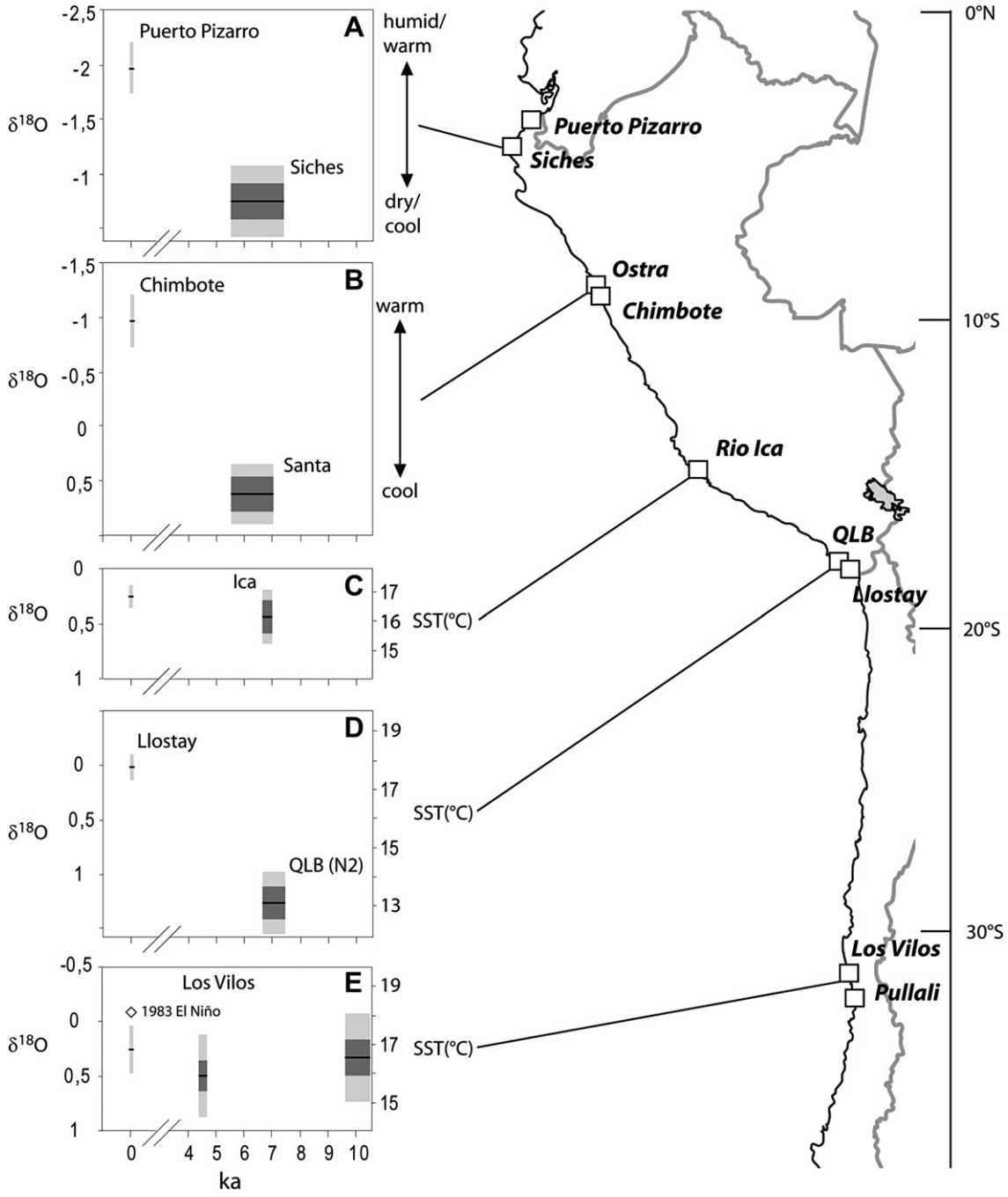

Fig. 2. Map of the south American Pacific coast showing the location of the modern and archaeological sites studied where mollusc shells were collected. For every location, annual mean isotopic values obtained from modern shells and fossil shells are compared. $\delta^{18}O$ values were corrected from ice volume effect as indicated in Table 1. Systematic errors (dark grey) include ice effect uncertainty and potential advective salinity changes. Statistical errors (light grey) depend on the sample size and proxy uncertainties and were estimated from Monte Carlo simulations (E). The Ostra value is an average of Perrier et al. (1994) values and Houk's (2002) values. The timescale corresponds to calibrated ages (Table 2).

Peru and lower valleys were not yet filled by sediment (Wells and Noller, 1999). Sea water could thus enter much further inland in the mid-Holocene, creating salinity gradients over several kilometres where fishes could have perhaps migrated. New elements are provided by the unpublished results of Nicholas (1996) and Houk (2002): isotopic data measured in mangrove mollusc shells from Siches clearly demonstrate cooler and/or drier conditions in the mid-Holocene (Table 3, Fig. 2). This result is consistent with the paleoclimatic records of the equatorial Pacific (Colinvaux, 1972; Koutavas et al., 2002; Kienast et al., 2006; Koutavas and Sachs, 2008) supporting La Niña-like mean conditions.

At Ostra, Sandweiss (1986) and Sandweiss and Richardson (1996) also concluded that the ocean was warmer throughout the year because of the presence of tropical mollusc species. However, several authors have argued that this presence in the mid-Holocene was due to a long sand spit enclosing a shallow bay with limited connection to the open sea where warm conditions could persist locally (De Vries and Wells, 1990; Perrier et al., 1994; De Vries et al., 1997). Substantially enriched isotopic values (Fig. 2) in fossil shells (including tropical species) (Perrier et al., 1994; Houk, 2002) have helped to solve this debate in that they can only be explained by evaporative conditions as observed in a shallow lagoon or by an

Table 2
Mesodesma donacium isotopic data.

Shell	Mean $\delta^{18}O$ (‰/V-PDB)	Number of years	Shell	Mean $\delta^{18}O$ (‰/V-PDB)	Number of years
Rio Ica, modern			*Rio Ica, Mid-Holocene*		
ICA-1	0.32	2	IN-N2-1	0.34	1.5
ICA-3	0.46	2	IN-N2-2	0.98	1
ICA-4	0.32	1.5	IN-N2-3	0.29	2
ICA-5	0.38	2	IN-N3-2	0.58	1
ICA-6	0.09	2	IN-N3-3	0.21	1
ICA-7	0.24	1	IN-N4-1	0.26	1
ICA-8	0.51	2.5	IN-N4-2	0.16	1
ICA-9	0.35	1	IN-N5-1	0.27	1
ICA-10	0.06	2	IN-N5-2	0.39	1
ICA-11	0.00	1.5	IN-N6-1	0.53	1.5
ICA-12	0.35	2	IN-N6-2	0.51	1.5
ICA-13	0.28	1	IN-N6-3	0.43	1.5
ICA-14	0.12	2	IN-N7-1	0.57	2
ICA-15	−0.04	1.5	IN-N7-2	0.67	1.5
ICA-16	0.32	1.5	IN-N7-3	0.48	1
			IN-N8-1	0.67	2
			IN-N8-2	0.61	2
			IN-N8-3	0.56	1.5
			IN-N9-1	0.47	1.5
			IN-N9-2	0.68	1.5
Llostay beach, modern			*QLB, Mid-Holocene*		
brmd24	0.27	2	N2i1	1.26	1
brmd25	0.07	1	N2i3	1.21	1
Lyl1	0.14	1.5	N2i8	1.04	1
Lymd2	0.12	1.5	N2i9	1.60	1
Lymd3	0.18	1	N2i13	1.22	1
Lymd4	0.06	1	N2i11	1.50	1
Lymd5	−0.22	1	N2i16	1.40	1
Lymd6	−0.05	1	N2i18	1.56	1.5
Lymd7	0.00	1	N2i19	1.03	1
Lymd8	−0.03	1	N2i20	1.30	1
Lymd9	0.55	1	N2i21	1.38	1
Lymd10	−0.18	1	N2i26	1.42	1
Lymd11	−0.07	1	N2i27	1.39	1
Lymd12	−0.19	1	N2i28	1.35	1.5
Lymd13	−0.19	1.5			
Lymd14	0.05	1			
Lymd15	−0.17	1			
Los Vilos, modern			*LV158, mid-Holocene*		
PLA-1	0.17	2	LV-158-N5_1	0.48	1
PLA-2	0.28	1	LV-158-N4_1	0.56	1
PLA-3	0.29	1.5	LV-158-N3_1	0.53	1
PLA-4	0.31	1	LV-158-N2_1	0.45	1
PLA-5	0.26	1	LV-158-N1_1	0.48	1
			LV 098B, Early Holocene		
Pullali, 1983			NAGB-N7_1	0.63	1
PU1	−0.09	1	NAGB-N9_1	0.60	1
			NAGB-N11_1	0.79	1
			NAGB-N13_1	0.66	1
			NAGB-N15_1	0.54	1

Table 3
Mollusk isotopic data from Perrier et al. (1994), Nicholas (1996), and Houk (2002). All shells are aragonitic.

Species	Ref. #	Mean $\delta^{18}O$ (‰/V-PDB)	Species	Ref. #	Mean $\delta^{18}O$ (‰/V-PDB)
Puerto Pizarro, modern			*Siches, mid-Holocene*		
C. subrugosa[b]	PT 1-14	−1.88	*C. subrugosa*[b]	PV 7-19 IB7	−0.60
C. subrugosa[b,c]	2PT1	−2.12	*C. subrugosa*[b]	PV 7-19 IIB3a	−0.90
A. tuberculosa[b]	AT 5-1	−1.95	*C. subrugosa*[b]	PV 7-19 IIB3b	−1.00
A. tuberculosa[b]	AT 5-2	−1.87	*A. tuberculosa*[b]	PV 7-19 IIB3a	−0.45
			A. tuberculosa[b]	PV 7-19 IIB3b	−0.10
			P. ecuatoriana[b]	PV 7-19 IB4bi	−0.60
			P. ecuatoriana[b]	PV 7-19 IB6b	−0.73
			P. ecuatoriana[b]	PV 7-19 IB7	−1.10
			P. ecuatoriana[b]	PV 7-19 IIB4a	−0.56
			P. ecuatoriana[b]	PV 7-19 IIB4b	−0.95
Chimbote, modern			*Santa, mid-Holocene*		
T. procerum[b,c]	TP 1-12	−1.11	*T. procerum*[c]	OBC V-1-C 2i-2ib	0.22
T. procerum[b]	3TP1-1b	−0.47	*C. broggi*[a]	CP-124	0.50
Samanco, modern			*C. broggi*[a]	CP-121	0.79
T. procerum[a]	CP-164.1	−0.69	*C. broggi*[a]	CP-104	0.93
T. procerum[a]	CP-164.2	−1.54	*C. broggi*[a]	CP-67	0.34
			C. broggi[a]	CP-126	0.96
			C. broggi[a]	CP-124	0.88
			C. broggi[a]	P-278	0.78
			T. procerum[a]	CP-120	1.03
			T. procerum[a]	CP-71	0.92
			T. procerum[a]	CP-124	1.09
			T. procerum[a]	CP-106	0.88
			T. procerum[a]	CP-164	−0.27
			T. dombei[a]	CP-126	0.70
			T. dombei[a]	P-279	0.53
			C. stercusmuscarum[a]	CP-124	1.59
			C. stercusmuscarum[a]	CP-113	1.57
			T. procerum[a]	CP-71	0.15
			T. procerum[a]	CP-106.1	0.00
			T. procerum[a]	CP-106.2	0.40
			T. procerum[a]	CP-120	0.13

[a] Analysed by Perrier et al. (1994).
[b] Analysed by Nicholas (1996).
[c] Analysed by Houk (2002).

extreme 6 °C cooling that tropical species could not cope with. These data indicate that the anomalous mollusc assemblages at Ostra do not reflect open sea conditions. Further south, between 15°S and 18°S, the coastal upwelling was also stronger as shown by cooler SSTs and increased marine reservoir ages (Fontugne et al., 2004). Terrestrial evidence for the increased influence of coastal fogs also supports this conclusion (cf. Fontugne et al., 1999). The cooling seems much larger at QLB than at Rio Ica (Fig. 2), which may indicate a spatial reorganization of coastal upwelling cells. Nearshore SST gradients along the Peruvian coast are more determined by the position of the upwelling centres than by latitude. For instance, despite the general latitudinal SST gradient, modern coastal SSTs are warmer at QLB (18°S) than at Rio Ica (15°S) because the former is located outside an upwelling cell and the latter inside.

It is interesting to note that the mid-Holocene was characterized in Peru as a period of low marine sedimentation rates and low productivity (Rein et al., 2005; Makou et al., 2010) despite stronger upwelling. Thus, millennial scale primary productivity changes off Peru would be more determined by the fertilization from continental input than by the upwelling intensity, as it was shown in Chile by Dezileau et al. (2004).

Paleoclimate records from the eastern equatorial Pacific associated with mollusc shell isotopic records from the Peruvian coast yield consistent results showing cooler mean conditions in the cold tongue and along the coast, characterizing a shallower mean position of the thermocline, increased wind stress and coastal upwelling, as observed today during La Niña conditions.

4.2. Chile–Peru coast

Paleoclimate records from the central coast of Chile yield a more complex picture. On one hand, fossil pollen records from continental archives clearly indicate strongly increased aridity during the mid-Holocene (Villagran and Varela, 1990; Maldonado and Villagrán, 2002, 2006; Villa-Martínez et al., 2003), consistent

Table 4
Data synthesis.

Reference		Site	Coordinates	Proxy	Results for the mid-Holocene
Eastern Pacific					
Koutavas et al. (2002)	1	V21-30	1°13′S; 89°40′W	Foram Mg/Ca	~1 °C cooler, La Niña-like
Koutavas and Sachs (2008)	1	V21-30	1°13′S; 89°40′W	$U^{K'}_{37}$ index	~0.1 °C cooler
	2	V19-27	0°28′S; 82°4′W	$U^{K'}_{37}$ index	~1 °C cooler
	3	V19-28	2°22′S; 84°39′W	$U^{K'}_{37}$ index	~0.5 °C cooler
	4	V19-30	3°23′S; 83°31′W	$U^{K'}_{37}$ index	~0.4 °C cooler
Kienast et al. (2006)	5	ME0005A-24JC	0°1,3′N; 86°27,8′W	Uk37	~1 °C cooler
Lea et al. (2006)	6	TR163-22	0°30.9′N; 92°23.9′W	Foram Mg/Ca	Similar temperature
Andrus et al. (2002)	7	Siches	4°30′S; 81°17′W	Otoliths $\delta^{18}O$	~3–4 °C warmer
Béarez et al. (2003) response to Andrus et al. (2002)					Light $\delta^{18}O$ values due to fish incursions into estuaries rather than warming.
Houk (2002)				Mollusk $\delta^{18}O$	Cooler and/or dryer conditions
Sandweiss and Richardson (1996)	8	Ostra	8°55′S; 78°38′W	Mollusk assemblages	Warmer
De Vries et al. (1997), response to Sandweiss and Richardson (1996)					Tropical molluscs presence were due to coastal lagoons rather than tropical mean conditions
Perrier et al. (1994)				Mollusk $\delta^{18}O$	Cool/dry or evaporative (lagoon) conditions
Fontugne et al. (2004)	9	QLB	18°1′S ; 70°50′W	Mollusk/charcoal ^{14}C	Increased marine reservoir age. Increased upwelling
This study	10	Rio Ica	14°52′S; 75°34′W	Mollusk $\delta^{18}O$	~1 °C cooler
	9	QLB	18°1′S; 70°50′W		~4 °C cooler
	11	Los Vilos	31°52′S; 71°31′W		~1 °C cooler
Mohtadi et al. (2004)	12	GeoB 7112-5	24°02′S; 70°49′W	Diatoms	Decreased productivity, higher rate of tropical–subtropical diatoms
Kaiser et al. (2008)	13	GeoB 7139-2	30°12′S; 71°59′W	UK′37 index	~2 °C warmer. Low vegetation. Increased productivity
Kim et al. (2002)	14	GIK 17748-2	32°45′S; 72°02′W	UK′37 index	~2–3 °C warmer
Ortlieb et al. (2011)	15	Multiple coastal sites from Southern Peru to Central Chile	16°20′S–23°34′S	Mollusk/charcoal ^{14}C	Increased marine reservoir age
Galapagos Islands					
Colinvaux (1972)	16	El Junco Lake	0°53′S; 89°28′W	Pollen	Lower lake level
Conroy et al. (2008)				Lake sediment	Drier conditions
Central Chile coast					
Villagran and Varela (1990)	17	Quereo	31°50′S; 71°30′W	Pollen and sediments	Aridity
	18	Quintero	32°47′S; 71°32′W		
Maldonado and Villagrán (2006)	19	Palo Colorado	32°05′S; 71°30′W	Pollen	Extreme aridity
Villa-Martínez et al. (2003)	20	Laguna Aculeo	33°50′S; 70°55′W	Pollen	Aridity
Jenny et al. (2002)				Lake sediments	Low lake level
South Brazil					
Behling et al. (2004)	21	Cambara do Sul	29°03′S; 50°06′W	Pollen	Warm and long dry season
Behling and Negrelle (2001)	22	Fazenda do Pinto	29°24′S; 50°34′W	Pollen	Warm and long dry season
Behling (1995)	23	Serra do Rio Rastro	28°23′S; 49°33′W	Pollen	Warm and long dry season
	24	Morro de Igreja	28°11′S; 49°52′W	Pollen	Warm and long dry season
	25	Serra de Boa vista	27°42′S; 49°09′W	Pollen	Warm and long dry season
Behling and Negrelle (2001)	26	Volta Vehla	26°04′S; 48°38′W	Pollen	Transition toward modern humid conditions
Behling (1997a)	27	Serra campos Gerais	24°40′S; 50°13′W	Pollen	Warm and long dry season
Behling (1998)	28	Botucatu	22°48′S; 48°23′W	Pollen	Warm and long dry season
Behling (1997b)	29	Morro de Itapeva	22°47′S; 45°32′W	Pollen	Warm and long dry season
Behling et al. (2007)	30	Serra do Bocaina	22°42′S; 44°34′W	Pollen	Transition toward modern humid conditions
Ledru et al. (2009)	31	Colonia	23°52′S; 46°42′W	Pollen	Drier
Zech et al. (2009)	32	Chasico	38°24′S; 62°51′W	Paleosoil	Drier
	33	D4	27°23′S; 55°31′W	Paleosoil	Drier
Iriarte 2006	34	Los Ajos	33°42′ S; 53°57′W	Pollen	Drier
Cruz et al. (2005)	35	Botuvera cave	27°13′S; 49°09′W	Speleothem	Weaker summer monsoon
Cruz et al. (2006)	36	Santana cave	24°31′S; 48°43′W	Speleothem	Weaker summer monsoon
Western slope of the central Andes					
Holmgren et al. (2001)	37	Multiple sites near Arequipa	*ca.* 16°10′S; *ca.* 71°48′W	Rodent middens	Wetter
Placzek et al. (2001)	38	Lake Aricota	17°22′S; 70°17′W	Diatomites	Wetter
Betancourt et al. (2000)	39	Tilomonte springs	23°40′S; 68°08′W	Wetland deposits	Wetter
Rech et al. (2003)	40	Quebrada Puripica	22°47′S; 48°05′W	Wetland deposits	Wetter

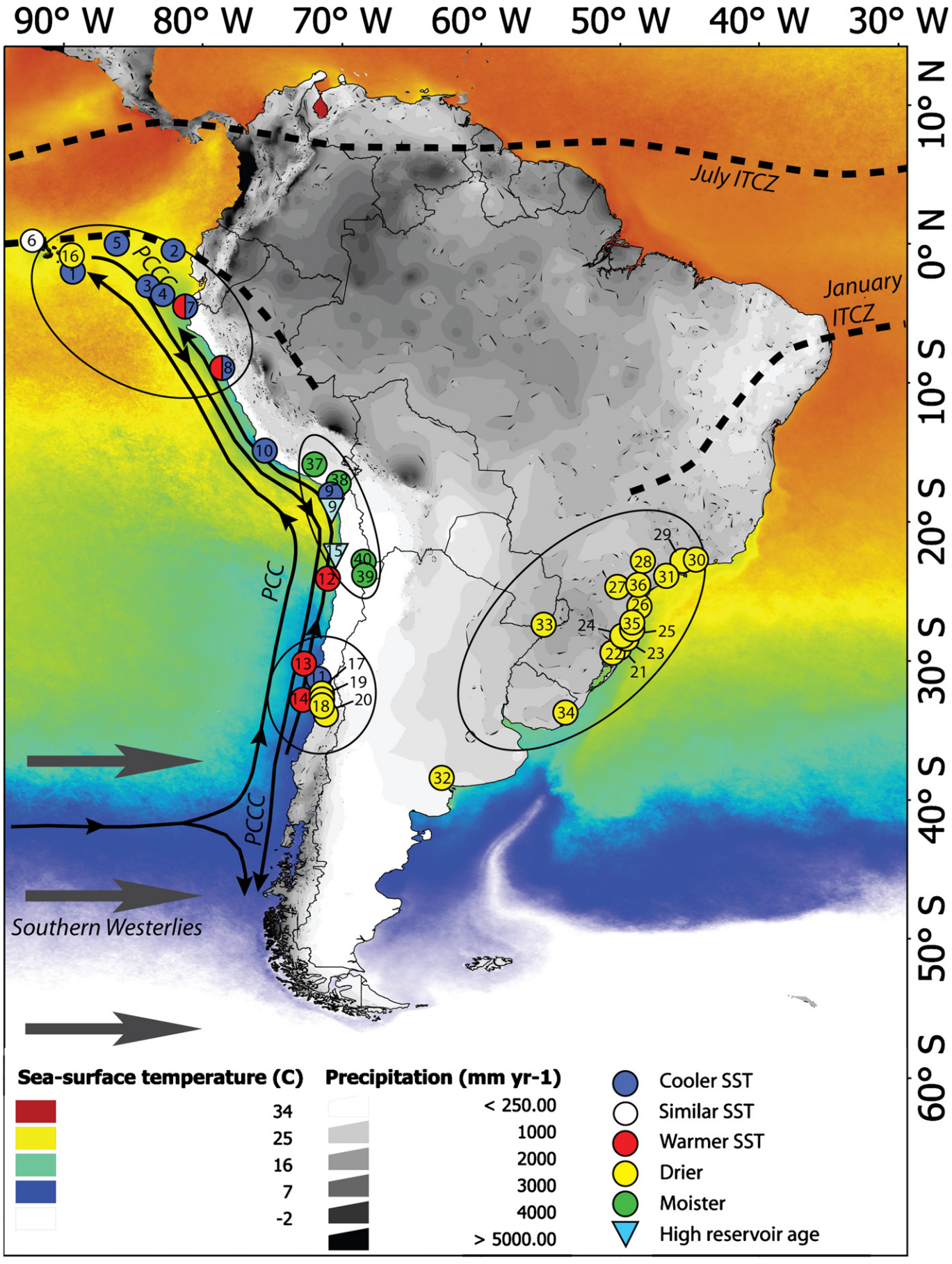
90° W
80° W
70° W
60° W
50° W
40° W
30° W
10° N
0° N
10° S
20° S
30° S
40° S
50° S
60° S
July ITCZ
January ITCZ
PCC
PCCC
Southern Westerlies
Sea-surface temperature (C)
34
25
16
7
-2
Precipitation (mm yr-1)
< 250.00
1000
2000
3000
4000
> 5000.00
Cooler SST
Similar SST
Warmer SST
Drier
Moister
High reservoir age

with stronger coastal upwelling as indicated by cooler waters nearshore (Fig. 2) and increased marine reservoir ages (Fontugne et al., 2004; Ortlieb et al., 2011). On the other hand, significantly warmer (2–3 °C) SSTs were reconstructed from diatom assemblages from marine sediment cores off Chile at 24°S (Mohtadi et al., 2004) and from alkenone unsaturation indices at 30°S (Kaiser et al., 2008), 32°S (Kim et al., 2002), and 41°S (Lamy et al., 2002). Non-thermal influences on alkenone SSTs, such as those presented in Prahl et al. (2006) and Popp et al. (2006), or a change in the season of maximum coccolithophorid production from winter to summer in this subtropical-to-mid-latitude region cannot explain the mid-Holocene warming observed in four sediment cores over 1100 km off the Chilean coast.

The alkenone-derived high SSTs close to, or within the direct influence of the coastal Chilean upwelling seem inconsistent with cooler conditions from southern Peru to the Galapagos, since these waters are connected through the Peru–Chile equatorward current (PCC) and the Peru–Chile poleward counter current (PCCC) (Fig. 3) that induce a continuity in the latitudinal SST gradient (Wyrtki, 1967; Strub et al., 1998). The overall conditions reconstructed seem robust but do not fit El Niño/La Niña-like patterns as observed today. The reconstructed pattern involving cooler waters nearshore and warmer conditions ~40 km offshore implies strengthened seaward SST gradients as observed today during the austral summer season (Strub et al., 1998). Evidence from other sectors of the southern hemisphere indicates that the southern westerlies and the subtropical front were displaced poleward during the mid-Holocene (Peeters et al., 2004), and by as much as 5° south along the Chilean coast (Verleye and Louwye, 2010). This increased distance from the westerly storm track added to the strengthened subtropical anticyclone appears to have resulted in extreme aridity in Central Chile (Maldonado and Villagrán, 2006).

The PCC is fed today by surface waters from the southern subtropical front, a latitudinal band comprised between 40°S and 45°S characterized by a strong latitudinal SST gradient overlapping southern subtropical waters and surface subantarctic waters (Strub et al., 1998). A possible effect of the mid-Holocene southward shift of the subtropical front is the increased relative influence of southern subtropical waters compared to subantarctic waters in the equatorward PCC, increasing thus the average temperature of the current. Warmer conditions prevailed on the continent both locally, as indicated by pedological studies (Veit, 1996), and regionally, as shown by Andean ice cores (Thompson et al., 1995, 1998). The resulting increased land–sea temperature difference would have modified the longshore windfields, contracting the coastal upwelling strip as described by Rutllant et al. (2003) and resulting in increased seaward SST gradient. This proposed scenario is still speculative and would need to be checked by additional SST reconstructions from alternative paleo-SST proxies from the Chilean margin, as well as paleo-SST reconstructions from the Peruvian margin. In the highly complex Chilean coastal oceanographic system, this apparently contradictory paleo-SST pattern could have been also the result of other mechanisms such as a change in the cloud cover-SST feedback.

4.3. Western slope of the Andes

While the Chilean coast experienced warm and arid conditions, wetter conditions have been reconstructed at mid-altitude (~2000–3300 m a.s.l.) on the nearby Andean slope from rodent middens and wetland deposits (Table 4, Fig. 3). There is a highly significant negative correlation between summer precipitation in the western Andes and SST anomalies in the eastern tropical Pacific (Garreaud, 1999; Vuille et al., 2000). During La Niña phases, upper troposphere easterlies are increased and favour summer precipitation in the western Andes by turbulent entrainment of lower-level winds, whereas westerlies anomalies during El Niño periods inhibit moisture advection from the east (Vuille et al., 2000). ^{14}C dated organic deposits indicate high lake level from 8 to 3 ka in the Salar de Atacama (Betancourt et al., 2000; Rech et al., 2003) and from 7 to 2.8 ka in southern Peru (Placzek et al., 2001). Based on an analogy with modern climate, these authors concluded to persistent La Niña-like mean conditions during the middle Holocene.

4.4. Southern Brazil

Rainfall variability in southern Brazil is strongly related to the eastern tropical Pacific. The Atlantic dipole influence on the precipitation is strong over the Amazon basin, but lower than the ENSO forcing in South Brazil according to a recent study (Pezzi and Cavalcanti, 2001). Actual precipitation exhibits weak seasonality in this area (Grimm, 2003). Total annual rainfall is around 1000 mm and distributed year-round, with summer rainfall (December–March) being related to the South American Monsoon convection and winter rainfall (June–September) being largely resulting from cyclonic extratropical influence (Grimm, 2003; Garreaud et al., 2009). Pollen records from southern Brazil suggest the permanence of a long dry season in the mid-Holocene, where there is today no dry season (Behling et al., 2004) and a strong depletion of the rainforest where the dry season is short (Ledru et al., 2009). The existence of a long dry season that strongly affected the vegetation suggests that winter rainfall favoured by El Niño conditions today were strongly reduced in the mid-Holocene. Araujo et al. (2005) attribute the relative scarcity of human occupation during this period – referred to as the "Archaic Gap" – to increased aridity. $\delta^{18}O$ records from speleothems from Botúvera Cave (Cruz et al., 2005) and Santana Cave (Cruz et al., 2006) show decreased monsoon rainfall in the early and mid-Holocene, likely as a result of weaker summer insolation in the southern hemisphere. Mid-Holocene aridity in southern Brazil is a very robust result supported by all the paleoclimate proxy records. Summer precipitation was likely reduced in response to weaker convection, whereas winter precipitation were almost suppressed by a strengthened Atlantic subtropical anticyclone associated to La Niña-like mean conditions revealed in the south eastern Pacific.

4.5. Middle Holocene teleconnections

How the average climate signal is influenced by the interannual to decadal variability is also an important issue. Several paleoclimatic studies suggest reduced El Niño activity during the mid-Holocene (Rodbell et al., 1999; Tudhope et al., 2001; Koutavas et al., 2006), which could partly contribute to a more La Niña-like average signal in the proxy records. However, reservoir ages and coastal SSTs reconstructed in Peru suggest that the coastal upwelling mean intensity was even stronger in the middle Holocene than during modern La Niña phases.

ENSO Teleconnections are barely stable at decadal timescale (Aceituno and Montecinos, 1993), and therefore important changes should be expected at millennial timescales. Atmospheric circulation and heat and moisture transport were deeply modified in the tropics during the mid-Holocene, and would have likely changed

Fig. 3. Map of South America with modern annual mean precipitation (gray scale) and modern annual mean SSTs (colour scale). Eastern Pacific currents, the modern position of the ITCZ and the southern Westerlies are indicated. Selected Regions with strong ENSO teleconnections are circled. Mid-Holocene sites are located with symbols for dry/humid, warm/cool, increased reservoir age, and identified with numbers reported in Table 4. (For interpretation of the references to colour in this figure legend, the reader is referred to the web version of this article).

the relationship between SSTs and precipitation over South America, as suggested by simulation experiments (Jorgetti et al., 2006). However, this synthesis of terrestrial proxy records provides a coherent picture of the South American regions mean climate during the mid-Holocene that appears very similar to a modern La Niña-like pattern, consistent with oceanic records from the Pacific. This consistency between the Eastern Pacific SST pattern and the continental precipitation pattern suggests that atmospheric teleconnections between the eastern tropical Pacific and the four studied regions were similar during the middle Holocene. The atmospheric and oceanic circulation in the eastern Pacific favoured aridity along the South American Pacific coast from central Chile to the Galapagos as well as in southern Brazil, and increased precipitation on the western slope of the Andes. This would not apply to regions such as the high Andes and northern South America which are under the strong influence of the ITCZ and the South American monsoon, which were strongly affected by seasonal insolation parameters.

5. Conclusions

New isotopic data presented here from the Peruvian and Chilean coast indicates that coastal SST changes during the mid-Holocene were ~1–4 °C cooler than today as a result of an intensified Southeast Pacific Subtropical Anticyclone, a strengthened Peru–Chile Current and increased coastal upwelling. Together with SST reconstructions from the Eastern Equatorial Pacific and with increased marine reservoir age reconstructed in Chile and Peru, these results support a persistent La Niña-like mean state in the south eastern Pacific during the middle Holocene. Warmer waters reconstructed off Chile from alkenones indicate increased seaward SST gradient, and a change in the complex coastal oceanic circulation along the Chilean coast. Most climate models simulations forced with mid-Holocene insolation yield cooling in the eastern tropical Pacific and increased zonal SST gradients (Bush, 1999; Clement et al., 1999; Otto-Bliesner, 1999; Liu et al., 2000; Zhao et al., 2005), and thus climate models and proxy data yield qualitatively consistent results in the Eastern Pacific.

Terrestrial proxy data were reviewed from four South American areas (Galapagos, the central Chilean coast, Southern Brazil, and the western slope of the central Andes) selected to differentiate between regional eastern tropical Pacific and global climate influences. They all indicate precipitation changes similar to modern La Niña anomalies, suggesting similar middle Holocene atmospheric teleconnections between these regions and the eastern tropical Pacific.

The middle-Holocene was a period of higher temperature in the northern hemisphere (Kaufman et al., 2004), primarily in response to high latitude orbital forcing. Although the mid-Holocene warming is not a perfect analogue to the actual greenhouse warming because different forcings are involved, the results presented here tend to support a La Niña-like response of the tropical Pacific to a warmer world. This speculative scenario is at odds with most model simulations but is supported by observations of strengthening trend in the coastal upwelling systems in California (Bakun, 1990; Schwing and Mendelssohn, 1997), Morocco (McGregor et al., 2007) and Chile (Vargas et al., 2007).

Acknowledgements

This material is based upon work supported by the Pérou-Sud project, the National Geographic Society under grant #8122-06, the Joint Institute for the Study of Atmosphere and Ocean through a postdoctoral fellowship, the U.S. National Science Foundation under Grant No. NSF-ATM-0811382, the U.S. National Oceanic and Atmospheric Administration under Grant No. NOAA-NA08OAR4310685, and the FONDECYT under grants #11070016 and #1080458. We are thankful to Danièle Lavallée, Michèle Julien, Fernanda Falabella, Orest E. Kawka. Thanks to Fredy Cardenas from IMARPE for providing oceanographic data. We are thankful to René Garreaud and two anonymous reviewers for helping improve the manuscript. This is the ISEM contribution 2011-017.

References

Aceituno, P., 1988. On the functioning of the southern oscillation in the South American sector. Part I: Surface climate. Monthly Weather Review 116, 505–524.

Aceituno, P., Montecinos, A., 1993. Análisis de la estabilidad de la relación entre la oscilación del sur y la precipitación en América del sur. Bulletin de l'Institut Français d'Etude Andines 22, 53–64.

Andrus, C.F.T., Crowe, D.E., Sandweiss, D.H., Reitz, E.J., Romanek, C.S., 2002. Otolith $\delta^{18}O$ record of mid-Holocene sea surface temperatures in Peru. Science 295, 1508–1511.

Andrus, C.F.T., Crowe, D.E., Sandweiss, D.H., Reitz, E.J., Romanek, C.S., Maasch, K.A., 2003. Response to comment on "Otolith $\delta^{18}O$ record of mid-Holocene sea surface temperatures in Peru". Science 299, 203b.

Araujo, A.G.M., Neves, W.A., Piló, L.B., Atui, J.P.V., 2005. Holocene dryness and human occupation in Brazil during the "Archaic Gap". Quaternary Research 64, 298–307.

Bakun, A., 1990. Global warming change and intensification of coastal ocean upwelling. Science 247, 198–201.

Barrionuevo, R., Marcial, R., 2006. Ecologia trofica de la fauna acuatica en el manglar de San Pedro – Sechura. Universalia 11, 44–56.

Béarez, P., DeVries, T.J., Ortlieb, L., 2003. Comment on "Otolith $\delta^{18}O$ record of mid-Holocene sea surface temperatures in Peru". Science 299, 203.

Behling, H., 1995. Investigations into the late Pleistocene and Holocene history of vegetation and climate in Santa Catarina (S Brazil). Vegetation History and Archaeobotany 4, 127–152.

Behling, H., 1997a. Late Quaternary vegetation, climate and fire history of the *Araucaria* forest and campos region from Serra Campos Gerais, Parana State (South Brazil). Review of Palaeobotany and Palynology 97, 109–121.

Behling, H., 1997b. Late Quaternary vegetation, climate and fire history from the tropical mountain region of Morro de Itapeva, SE Brazil. Palaeogeography, Palaeoclimatology, Palaeoecology 129, 407–422.

Behling, H., 1998. Late Quaternary vegetational and climatic changes in Brazil. Review of Palaeobotany and Palynology 99, 143–156.

Behling, H., Negrelle, R.R.B., 2001. Tropical rain forest and climate dynamics of the Atlantic Lowland, Southern Brazil, during the Late Quaternary. Quaternary Research 56, 383–389.

Behling, H., Pillar, V.D., Orlóci, L., Bauermann, S.G., 2004. Late Quaternary Araucaria forest, grassland (Campos), fire and climate dynamics, studied by high-resolution pollen, charcoal and multivariate analysis of the Cambará do Sul core in southern Brazil. Palaeogeography, Palaeoclimatology, Palaeoecology 203, 277–297.

Behling, H., Dupont, L., DeForest Safford, H., Wefer, G., 2007. Late Quaternary vegetation and climate dynamics in the Serra da Bocaina, southeastern Brazil. Quaternary International 161, 22–31.

Betancourt, J.L., Latorre, C., Rech, J.A., Quade, J., Rylander, K.A., 2000. A 22,000-year record of monsoonal precipitation from northern Chile's Atacama desert. Science 289.

Bush, A.B.G., 1999. Assessing the impact of Mid-Holocene insolation on the atmosphere–ocean system. Geophysical Research Letters 26, 99–102.

Carré, M., 2007. El mes de recolección de la macha (*Mesodesma donacium*) determinado por sus líneas de crecimiento: aplicaciones arqueológicas. Bulletin de l'Institut Français d'Etudes Andines 36, 299–304.

Carré, M., Bentaleb, I., Blamart, D., Ogle, N., Cardenas, F., Zevallos, S., Kalin, R.M., Ortlieb, L., Fontugne, M., 2005a. Stable isotopes and sclerochronology of the bivalve *Mesodesma donacium*: potential application to Peruvian paleoceanographic reconstructions. Palaeogeography, Palaeoclimatology, Palaeoecology 228, 4–25.

Carré, M., Bentaleb, I., Fontugne, M., Lavallée, D., 2005b. Strong El Niño events during the early Holocene: stable isotope evidence from Peruvian sea-shells. The Holocene 15, 42–47.

Carré, M., Klaric, L., Lavallée, D., Julien, M., Bentaleb, I., Fontugne, M., Kawka, O., 2009. Insights into early Holocene hunter–gatherer mobility on the Peruvian Southern Coast from mollusk gathering seasonality. Journal of Archaeological Science 36, 1173–1178.

Clement, A.C., Seager, R., Cane, M.A., 1999. Orbital controls on the El Niño/Southern oscillation and the tropical climate. Paleoceanography 14, 441–456.

Colinvaux, P.A., 1972. Climate and the Galapagos Islands. Nature 240, 17–20.

Conroy, J.L., Overpeck, J.T., Cole, J.E., Shanahan, T.M., Steinitz-Kannan, M., 2008. Holocene changes in eastern Pacific climate inferred from a Galápagos lake sediment record. Quaternary Science Reviews 27, 1166–1180.

Cruz, F.W., Burns, S.J., Karmann, I., Sharp, W.D., Vuille, M., Cardoso, A.O., Ferrari, J.A., Silvia Dias, P.L., Viana, O., 2005. Insolation-driven changes in atmospheric circulation over the past 116,000 years in subtropical Brazil. Nature 434, 63–66.

Cruz, J.F.W., Burns, S.J., Karmann, I., Sharp, W.D., Vuille, M., 2006. Reconstruction of regional atmospheric circulation features during the late Pleistocene in

subtropical Brazil from oxygen isotope composition of speleothems. Earth and Planetary Science Letters 248, 495–507.
Delaygue, G., Jouzel, J., Dutay, J.-C., 2000. Oxygen 18-salinity relationship simulated by an oceanic general circulation model. Earth and Planetary Science Letters 178, 113–123.
De Vries, T.J., Wells, L.E., 1990. Thermally anomalous Holocene molluscan assemblages from coastal Peru: evidence for paleogeographic, not climatic change. Palaeogeography, Palaeoclimatology, Palaeoecology 81, 11–32.
De Vries, T.J., Ortlieb, L., Diaz, A., Wells, L., Hillaire-Marcel, C., Wells, L.E., Noller, J.S., Sandweiss, D.H., Richardson III, J.B., Reitz, E.J., Rollins, H.B., Maasch, K.A., 1997. Determining the early history of El Nino. Science 276, 965–967.
Dezileau, L., Ulloa, O., Hebbeln, D., Lamy, F., Reyss, J.-L., Fontugne, M., 2004. Iron control of past productivity in the coastal upwelling system off the Atacama desert, Chile. Paleoceanography 19, PA3012. doi:10.1029/2004PA001006.
Engel, F., 1957. Early sites on the Peruvian coast. Southwestern Journal of Anthropology 13, 54–68.
Epstein, S., Buchsbaum, R., Lowenstam, H.A., Urey, H.C., 1953. Revised carbonate-water isotopic temperature scale. Bulletin of the Geological Society of America 64, 1315–1326.
Fleitmann, D., Burns, S.J., Mudelsee, M., Neff, U., Kramers, J., Mangini, A., Matter, A., 2003. Holocene forcing of the Indian monsoon recorded in a stalagmite from southern Oman. Science 300, 1737–1739.
Fontugne, M., Usselmann, P., Lavallée, D., Julien, M., Hatté, C., 1999. El Nino variability in the coastal desert of southern Peru during the mid-Holocene. Quaternary Research 52, 171–179.
Fontugne, M., Carré, M., Bentaleb, I., Julien, M., Lavallée, D., 2004. Radiocarbon reservoir age variations in the south Peruvian upwelling during the Holocene. Radiocarbon 46, 531–537.
Garreaud, R.D., 1999. Multiscale analysis of the summertime precipitation over the Central Andes. Monthly Weather Review 127, 901–921.
Garreaud, R.D., Vuille, M., Compagnucci, R., Marengo, J., 2009. Present-day South American climate. Palaeogeography, Palaeoclimatology, Palaeoecology 281, 180–195.
Grimm, A.M., 2003. The El Niño impact on the summer monsoon in Brazil: regional processes versus remote influences. Journal of Climate 16, 263–280.
Grimm, A.M., Tedeschi, R.G., 2009. ENSO and extreme rainfall events in South America. Journal of Climate 22, 1589–1609.
Grimm, A.M., Barros, V.R., Doyle, M.E., 2000. Climate variability in Southern South America associated with El Niño and La Niña Events. Journal of Climate 13, 35–58.
Grossman, E.L., Ku, T.-L., 1986. Oxygen and carbon fractionation in biogenic aragonite: temperature effect. Chemical Geology 59, 59–74.
Haug, G.H., Hughen, K.A., Sigman, D.M., Peterson, L.C., Röhl, U., 2001. Southward migration of the intertropical convergence zone through the Holocene. Science 293, 1304–1308.
Holmgren, C.A., Betancourt, J.L., Rylander, K.A., Roque, J., Tovar, O., Zeballos, H., Linares, E., Quade, J., 2001. Holocene vegetation history from fossil rodent middens near Arequipa, Peru. Quaternary Research 56, 242–251.
Houk, S.D., 2002. Growth increment analysis of marine bivalve from the north coast of Peru. University of Maine, Unpublished thesis, pp.133.
Hughen, K.A., Baillie, M.G.L., Bard, E., Beck, J.W., Bertrand, C.J.H., Blackwell, P.G., Buck, C.E., Burr, G.S., Cutler, K.B., Damon, P.E., Edwards, R.L., Fairbanks, R.G., Friedrich, M., Guilderson, T.P., Kromer, B., McCormac, G., Manning, S., Bronk Ramsey, C., Reimer, P.J., Reimer, R.W., Remmele, S., Southon, J.R., Stuiver, M., Talamo, S., Taylor, F.W., van der Plicht, J., Weyhenmeyer, C.E., 2004. Marine04 marine radiocarbon age calibration, 0–26 Cal kyr BP. Radiocarbon 46, 1059–1086.
Iriarte, J., 2006. Vegetation and climate change since 14,810 ^{14}C yr B.P. in southeastern Uruguay and implications for the rise of early Formative societies. Quaternary Research 65, 20–32.
Jackson, D., Méndez, C., 2005. Reocupando el espacio: Historia de un asentamiento multicomponente, sus relaciones inter-sitios y los cambios paleoambientales de la costa del Choapa. Revista Werken 6, 5–14.
Jenny, B., Valero-Garcés, B.L., Villa-Martínez, R., Urrutia, R., Geyh, M., Veit, H., 2002. Early to Mid-Holocene aridity in central Chile and the southern westerlies: the Laguna Aculeo record (34°S). Quaternary Research 58, 160–170.
Jorgetti, T., Silva Dias, P.L., Braconnot, P., 2006. Review of: El Niño influence over South America during the mid-Holocene. Advances in Geosciences 6, 279–282.
Kaiser, J., Schefuß, E., Lamy, F., Mohtadi, M., Hebbeln, D., 2008. Glacial to Holocene changes in sea surface temperature and coastal vegetation in north central Chile: high versus low latitude forcing. Quaternary Science Reviews 27, 2064–2075.
Kaufman, D.S., Ager, T.A., Anderson, N.J., Anderson, P.M., Andrews, J.T., Bartlein, P.J., Brubaker, L.B., Coats, L.L., Cwynar, L.C., Duvall, M.L., Dyke, A.S., Edwards, M.E., Eisner, W.R., Gajewski, K., Geirsdóttir, A., Hu, F.S., Jennings, A.E., Kaplan, M.R., Kerwin, M.W., Lozhkin, A.V., MacDonald, G.M., Miller, G.H., Mock, C.J., Oswald, W.W., Otto-Bliesner, B.L., Porinchu, D.F., Rühland, K., Smol, J.P., Steig, E.J., Wolfe, B.B., 2004. Holocene thermal maximum in the western Arctic (0–180°W). Quaternary Science Reviews 23, 529–560.
Kienast, M., Kienast, S., Calvert, S.E., Eglinton, T.I., Mollenhauer, G., François, R., Mix, A.C., 2006. Eastern Pacific cooling and Atlantic overturning circulation during the last deglaciation. Nature 443, 846–849.
Kim, J.-H., Schneider, R.R., Hebbeln, D., Müller, P.J., Wefer, G., 2002. Last deglacial sea-surface temperature evolution in the Southeast Pacific the South American continent. Quaternary Science Reviews 21, 2085–2097.
Koutavas, A., Sachs, J.P., 2008. Northern timing of deglaciation in the eastern equatorial Pacific from alkenone paleothermometry. Paleoceanography 23. doi:10.1029/2008PA001593.
Koutavas, A., Lynch-Stieglitz, J., Marchitto Jr., T.M., Sachs, J.P., 2002. El Niño-like pattern in ice age tropical sea surface temperature. Science 297, 226–230.
Koutavas, A., deMenocal, P.B., Olive, G.C., Lynch-Stieglitz, J., 2006. Mid-Holocene El Niño-Southern Oscillation (ENSO) attenuation revealed by individual foraminifera in eastern tropical Pacific sediments. Geology 34, 993–996.
Lambeck, K., Chappell, J., 2001. Sea level change through the last glacial cycle. Science 292, 679–686.
Lamy, F., Hebbeln, D., Röhl, U., Wefer, G., 2001. Holocene rainfall variability in southern Chile: a marine record of latitudinal shifts of the southern westerlies. Earth and Planetary Science Letters 185, 369–382.
Lamy, F., Rühlemann, C., Hebbeln, D., Wefer, G., 2002. High- and low-latitude climate control on the position of the southern Peru–Chile current during the Holocene. Paleoceanography 17 (16), 1–10.
Lavallée, D., Julien, M., Béarez, P., Usselman, P., Fontugne, M., Bolaños, A., 1999. Pescadores-recolectores arcaicos del extremo-sur Peruano. Excavaciones en la Quebrada de los Burros (Departamento de Tacna). Primeros resultados 1995–1997. Bulletin de l'Institut Français d'Etude Andines 28, 13–52.
Lea, D.W., Pak, D.K., Belanger, C.L., Spero, H.J., Hall, M.A., Shackleton, N.J., 2006. Paleoclimate history of Galápagos surface waters over the last 135,000 yr. Quaternary Science Reviews 25, 1152–1167.
Ledru, M.-P., Mourguiart, P., Riccomini, C., 2009. Related changes in biodiversity, insolation and climate in the Atlantic rainforest since the last interglacial. Palaeogeography, Palaeoclimatology, Palaeoecology 271, 140–152.
Lenters, J.D., Cook, K.H., 1999. Summertime precipitation variability over South America: role of the large-scale circulation. Monthly Weather Review 127, 409–431.
Liu, Z., Kutzbach, J., Wu, L., 2000. Modeling climate shift of El Nino variability in the Holocene. Geophysical Research Letters 27, 2265–2268.
Makou, M.C., Eglinton, T.I., Oppo, D.W., Hughen, K.A., 2010. Postglacial changes in El Niño and La Niña behavior. Geology 38, 43–46.
Maldonado, A., Villagrán, C., 2002. Paleoenvironmental changes in the semiarid coast of Chile (~32°S) during the last 6200 cal years inferred from a swamp-forest pollen record. Quaternary Research 58, 130–138.
Maldonado, A., Villagrán, C., 2006. Climate variability over the last 9900 cal yr BP from a swamp forest pollen record along the semiarid coast of Chile. Quaternary Research 66, 246–258.
McCormac, F.G., Hogg, A.G., Blackwell, P.G., Buck, C.E., Higham, T.F.G., Reimer, P.J., 2004. SHCal04 southern hemisphere calibration, 0–11.0 Cal kyr BP. Radiocarbon 46, 1087–1092.
McGregor, H.V., Dima, M., Fischer, H.W., Mulitza, S., 2007. Rapid 20th-century increase in coastal upwelling off Northwest Africa. Science 315, 637–639.
Mitchell, T.P., Wallace, J.M., 1992. The annual cycle in equatorial convection and sea surface temperature. Journal of Climate 5, 1140–1156.
Mohtadi, M., Romero, O.E., Hebbeln, D., 2004. Changing marine productivity off northern Chile during the past 19000 years: a multivariable approach. Journal of Quaternary Science 19, 347–360.
Montecinos, A., Aceituno, P., 2003. Seasonality of the ENSO-related rainfall variability in central Chile and associated circulation anomalies. Journal of Climate 16, 281–296.
Montecinos, A., Diaz, A., Aceituno, P., 2000. Seasonal diagnostic and predictability of rainfall in subtropical South America based on tropical Pacific SST. Journal of Climate 13, 746–758.
Nicholas, S.L., 1996. Implications of the stable isotopes from marine shells for the mid-Holocene paleoclimate of the north Coast of Peru. University of Maine, Unpublished thesis.
Ortlieb, L., Vargas, G., Saliège, J.-F., 2011. Marine radiocarbon reservoir effect along the northern Chile-southern Peru coast (14–24°S) throughout the Holocene. Quaternary Research 75, 91–103.
Otto-Bliesner, B.L., 1999. El Niño/La Niña and Sahel precipitation during the middle Holocene. Geophysical Research Letters 26, 87–90.
Peeters, F.J.C., Acheson, R., Brummer, G.-J.A., de Ruijter, W.P.M., Schneider, R.R., Ganssen, G.M., Ufkes, E., Kroon, D., 2004. Vigorous exchange between the Indian and Atlantic oceans at the end of the past five glacial periods. Nature 430, 661–665.
Perrier, C., Hillaire-Marcel, C., Ortlieb, L., 1994. Paléogéographie littorale et enregistrement isotopique (13C, 18O) d'évènements de type El Niño par les mollusques Holocènes et récents du Nord-Ouest Péruvien. Géographie Physique et Quaternaire 48, 23–38.
Pezzi, L.P., Cavalcanti, I.F.A., 2001. The relative importance of ENSO and tropical Atlantic sea surface temperature anomalies for seasonal precipitation over South America: a numerical study. Climate Dynamics 17, 205–212.
Placzek, C., Quade, J., Betancourt, J.L., 2001. Holocene lake-level fluctuations of lake Aricota, southern Peru. Quaternary Research 56, 181–190.
Popp, B.N., Prahl, F.G., Wallsgrove, R.J., Tanimoto, J., 2006. Seasonal patterns of alkenone production in the subtropical oligotrophic North Pacific. Paleoceanography 21. doi:10.1029/2005PA001165.
Prahl, F.G., Mix, A.C., Sparrow, M.A., 2006. Alkenone paleothermometry: biological lessons from marine sediment records off western South America. Geochimica et Cosmochimica Acta 70, 101–117.
Rech, J.A., Pigati, J.S., Quade, J., Betancourt, J.L., 2003. Re-evaluation of mid-Holocene deposits at Quebrada Puripica, northern Chile. Palaeogeography, Palaeoclimatology, Palaeoecology 194, 207–222.
Rein, B., Lückge, A., Reinhardt, L., Sirocko, F., Wolf, A., Dullo, W.-C., 2005. El Niño variability off Peru during the last 20,000 years. Paleoceanography 20. doi:10.1029/2004PA001099.

Rodbell, D.T., Seltzer, G.O., Anderson, D.M., Abbott, M.B., Enfield, D.B., Newman, J.H., 1999. An ~15,000-year record of el nino driven alluviation in southwestern Ecuador. Science 283, 516–520.

Rutllant, J.A., Fuenzalida, H., Aceituno, P., 2003. Climate dynamics along the arid northern coast of Chile: the 1997–1998 DinÃ¡mica del Clima de la Region de Antofagasta (DICLIMA) experiment. Journal of Geophysical Research 108.

Sandweiss, H.D., 1986. The beach ridges at Santa, Peru: El Niño, uplift, and prehistory. Geoarchaeology 1, 17–28.

Sandweiss, D.H., Richardson, J.B., 1996. Geoarcheological evidence from Peru for a 5000 years B.P. onset of El Nino. Science 273, 1531–1533.

Schwing, F.B., Mendelssohn, R., 1997. Increased coastal upwelling in the California current system. Journal of Geophysical Research 102, 3421–3438.

Strub, P.T., Mesias, J.M., Montecino, V., Rutllant, J., Salinas, S., 1998. Coastal ocean circulation off western South America. In: Robinson, A.R., Brink, K.H. (Eds.), The Global Coastal Ocean. Regional Studies and Syntheses. Wiley, New York, pp. 273–315.

Stuiver, M., Reimer, P., 1993. Extended ^{14}C database and revised CALIB radiocarbon calibration program. Radiocarbon 35, 215–230.

Takahashi, K., Battisti, D.S., 2007. Processes controlling the mean tropical Pacific precipitation pattern: I. The Andes and the Eastern Pacific ITCZ. Journal of Climate 20, 3434–3451.

Thompson, L.G., Mosley-Thompson, E., Davis, M.E., Lin, P.-N., Henderson, K.A., Cole-Dai, J., Bolzon, J.F., Liu, K.-B., 1995. Late glacial stage and Holocene tropical ice core records from Huascaran, Peru. Science 269, 46–50.

Thompson, L.G., Davis, M.E., Mosley-Thompson, E., Sowers, T.A., Henderson, K.A., Zagorodnov, V.S., Lin, P.-N., Mikhalenko, V.N., Campen, R.K., Bolzan, J.F., Cole-Dai, J., Francou, B., 1998. A 25,000-year tropical climate history from Bolivian ice-cores. Science 282, 1858–1864.

Tudhope, A.W., Chilcot, C.P., McCulloch, M.T., Cook, E.R., et al., 2001. Variability in the El-Niño Southern oscillation through a Glacial–interglacial cycle. Science 291, 1511–1517.

Vargas, G., Pantoja, S., Rutllant, J.A., Lange, C.B., Ortlieb, L., 2007. Enhancement of coastal upwelling and interdecadal ENSO-like variability in the Peru–Chile Current since late 19th century. Geophysical Research Letters 34. doi:10.1029/2006GL028812.

Veit, H., 1996. Southern Westerlies during the Holocene deduced from geomorphological and pedological studies in the Norte Chico, Northern Chile (27–33°S). Palaeogeography, Palaeoclimatology, Palaeoecology 123, 107–119.

Verleye, T.J., Louwye, S., 2010. Late Quaternary environmental changes and latitudinal shifts of the Antarctic Circumpolar Current as recorded by dinoflagellate cysts from offshore Chile (41°S). Quaternary Science Reviews 29, 1025–1039.

Villagran, C., Varela, J., 1990. Palynological evidence for increased aridity on the central Chilean coast during the Holocene. Quaternary Research 34, 198–207.

Villa-Martínez, R., Villagrán, C., Jenny, B., 2003. The last 7500 cal yr B.P. of westerly rainfall in Central Chile inferred from a high-resolution pollen record from Laguna Aculeo (34°S). Quaternary Research 60, 284–293.

Vuille, M., Bradley, R.S., Keimig, F., 2000. Interannual climate variability in the Central Andes and its relation to tropical Pacific and Atlantic forcing. Journal of Geophysical Research 105, 12447–12460.

Wang, Y., Cheng, H., Edwards, R.L., He, Y., Kong, X., An, Z., Wu, J., Kelly, M.J., Dykoski, C.A., Li, X., 2005. The Holocene Asian monsoon: links to solar changes and north Atlantic climate. Science 308, 854–857.

Wells, L.E., Noller, J.S., 1999. Holocene coevolution of the physical landscape and human settlement in northern coastal Peru. Geoarchaeology 14, 755–789.

Wyrtki, K., 1967. Circulation and water masses in the equatorial Pacific ocean. International Journal of Oceanology & Limnology 1, 117–147.

Zech, W., Zech, M., Zech, R., Peinemann, N., Morras, H.J.M., Moretti, L., Ogle, N., Kalim, R.M., Fuchs, M., Schad, P., Glaser, B., 2009. Late Quaternary palaeosol records from subtropical (38°S) to tropical (16°S) South America and palaeoclimatic implications. Quaternary International 196, 107–120.

Zhao, Y., Braconnot, P., Marti, O., Harrison, S.P., Hewitt, C., Kitoh, A., Liu, Z., Mikolajewicz, U., Otto-Bliesner, B., Weber, S.L., 2005. A multi-model analysis of the role of the ocean on the African and Indian monsoon during the mid-Holocene. Climate Dynamics 25, 777–800.